Comparison of atmospheric transparency in Modtran and LibRadTran

S. Dagoret-Campagne[1] and K. Gilmore[2]
(LSST Dark Energy Science Collaboration)

[1] *LAL, Univ. Paris-Sud, CNRS/IN2P3, Université Paris-Saclay, Orsay, France*
[2] *SLAC National Accelerator Laboratory, Menlo Park, CA 94025, USA*

(Dated: December 21, 2018, version : V1.4, DESC-LSST-Note-LAL-2018-09-002)

In this study, optical atmospheric transmission characteristics between Modtran (MT) and LibRadTran (RT) in the LARGE SYNOPTIC SURVEY TELESCOPE (LSST) passband filters (U, G, R, I, Z, Y) are compared using identical data sets, to determine if the two radiative transfer packages produce different results.

1. Introduction

Reliable and realistic atmospheric transmission models are required to achieve millimag photometric calibration at the LSST. Atmospheric transmission transport codes provide accurate models that have been studied over several decades by earth sciences. However, slight discrepancies in radiative transfer equations and models of various packages may have an impact on photometric calibration accuracy. In this report, a comparison is made between the atmospheric transmission predicted by two radiative transfer packages: Modtran (3), (2) (version 5) and LibRadTran (5) (version v2.0.1).

The prediction of air transparency from an atmospheric transmission model depends on the observational altitude, airmass, atmospheric vertical profiles of pressure and temperature as well as vertical distribution of the atmospheric chemical component which all induce radiative absorption at some level. Therefore, the model comparison must be performed at similar airmass and various altitudes ($h = 2.7$ km) to obtain a similar atmospheric chemical element vertical profile. The US Standard atmospheric profile (4) is used as a realistic model with all variable parameters that are consistent with the LSST site. For this study, all parameters of the visible transmission curve do not have to be exactly reproduced but their averages inside a broad band filter of LSST must be preserved. The most relevant random parameters for MT/RT atmospheric models are precipitable water vapor (*pwv*) and ozone (*ozone*).

In this study, we do not consider aerosol variations or grey attenuation due to clouds. These parameters both have their own physical phenomenon independent of the core physical atmospheric models based on molecular scattering on air molecules (Rayleigh scattering) and on molecular absorption mostly with *oxygen*, *ozone* and precipitable water vapor.

For this exercise, the absolute value of *pwv* or *ozone* in Modtran or LibRadTran is not required because a function can be defined relating these two parameters in both the MT and RT solvers. Because of this, the predicted atmospheric transmission residuals will remain homogeneous within the required millimag accuracy. What matters in this case is the consistency of the prediction for any airmass. When choosing any light transmission curve at airmass $z = z_1$, reproduced by estimating atmospheric parameters $\{PMT\}$ in Modtran and by parameters $\{PRT\}$ in LibRadTran, this process must lead to the prediction of the transmission curve at any other airmass $z = z_2$ for the same parameters.

Because the LSST makes photometric measurements through broadband filters, the comparison will include the experimental magnitudes of astronomical objects through Modtran and LibRadTran, for all filters, at any airmass.

The investigation asks the following questions :

- Do atmospheric models implemented in Modtran/LibRadTran show significant magnitude biases in the LSST filters ?

- Can LibRadTran atmospheric parameters be tuned to exactly reproduce that of the MT parameters ?
- And, if so, what are the minimum residual magnitude errors achievable ?

In section 1, transmission curves for the analysis are shown. Modtran data available for this study are shown in Figure 1.a as transmission curves between 300 nm and 1200 nm for airmass between 1 and 2.5, in 0.1 steps, inclusive. The variable atmospheric parameters in Modtran have been chosen for $pwv = 4mm$ and $ozone = 300DbU$[1]. Figure 1.b shows LibRadTran atmospheric transmission curves at airmass $z = 1$ when varying *pwv* from 0 mm to 10 mm. In this way, one can easily identify the four wavelength domains corresponding to the water absorption bands. Similarly, Figure 1.c shows LibRadTran atmospheric transmission curves at airmass $z = 1.2$ when varying the *ozone* in realistic ranges from 250 Dobson Units (DbU) to 440 DbU. Figure 1.c also shows the *ozone* absorption band at a wavelength of about 600 nm called the Chappuis band[2] as well as the strong absorption cutoff below the Huggins band[3] at 360 nm.

An approximate comparison without variable parameter tuning (*pwv* and *ozone*) is shown in Figure 2 as the ratio of the transmission curve (Modtran/LibRadTran) in wavelength bins of 1 nm width, for the same airmass ranging from $z = 1.0$ to 2.5. Identification of the slight *ozone* discrepancy for both the Chappuis and Huggins bands is seen as well as the precipitable water vapor regions. This plot, however, does not show the level of discrepancy and impact on the magnitudes in the LSST broad band filters. Further studies will be required to determine if a significant magnitude bias exists. It can be seen that the transmission curves in the Rayleigh scattering region between 340 nm and 500 nm are well aligned indicating Modtran and LibRadTran produce almost identical atmospheric depths and molecular scattering as implemented by their respective radiative transfer equations. In this note, the question of magnitude bias is addressed to evaluate the photometric systematic errors when choosing one or the other atmospheric models.

In Section 2, methods are developed to evaluate magnitudes in each LSST filter and how LibRadTran atmospheric parameters can be tuned in a way that LibRadTran magnitudes

[1] A Dobson Unit is a unit of measurement for the total amount of ozone in the atmosphere above a point on the earth's surface, one Dobson unit being equivalent to a layer of pure ozone 0.01 mm thick at standard temperature and pressure.

[2] The Chappuis Band is a spectroscopic feature of the *ozone* molecule with considerable structure related to vibrational levels in the ozone molecule occurring at a wavelength around 600 nm, or an energy of 2 eV. These absorption bands lead to photodissociation of an ozone molecule into an O_2 molecule and an *oxygen*atom and are used to measure *ozone* in the atmosphere.

[3] The Huggins Band is a very strong absorption band of *ozone*lying approximately between 310 and 340 nm.

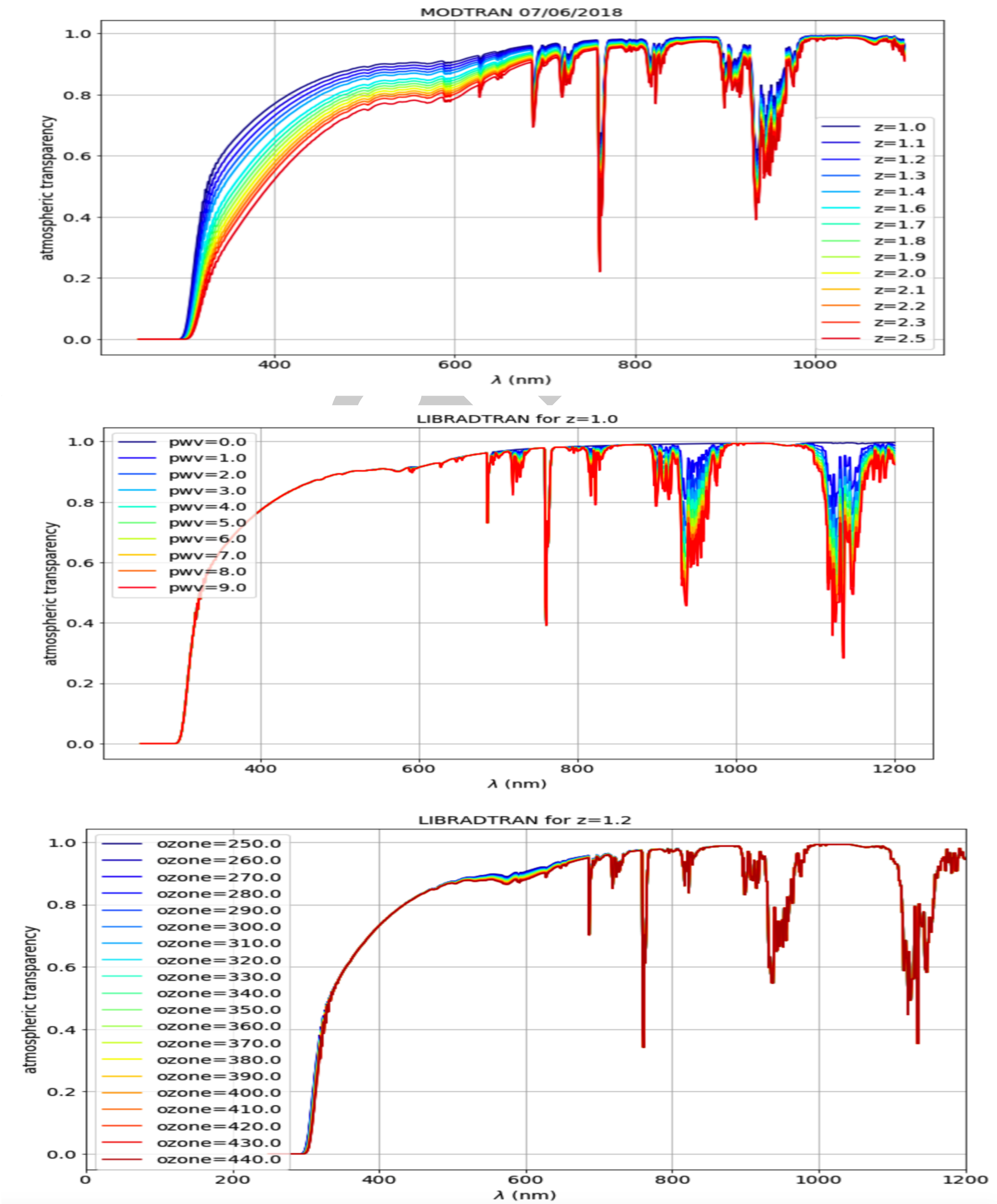

Figure 1. Atmospheric transmission : a) (top) Modtran for airmass $z = 1, ..2.5$. b) (middle) LibRadTran at airmass $z = 1$, when varying *pwv* from 0 to 10 mm. c) (bottom) LibRadTran at airmass $z = 1.2$, when varying *ozone* from 250 to 440 Dobson Unit.

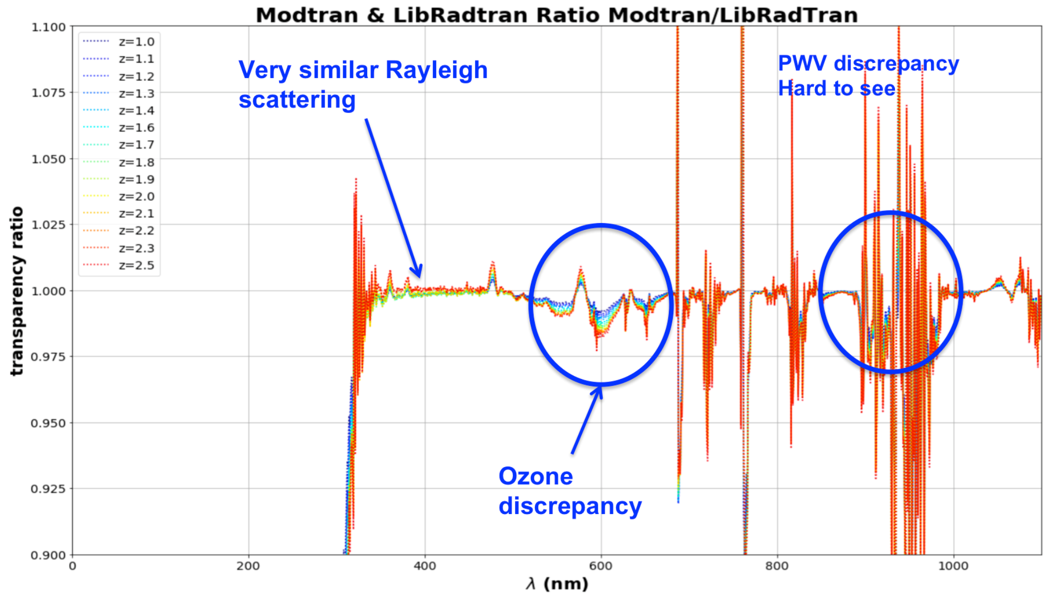

Figure 2. Initial comparison of Modtran and LibRadTran without matching atmospheric parameters *pwv* and *ozone* : transmission curves ratio.

match those of Modtran. The results of the analysis of magnitude differences in each filter are presented in Section 3. A discussion about magnitude discrepancies in some of the filters is then presented in Section 4.

2. Methods

2.1. Magnitude Calculation

The method used to evaluate the Modtran/LibRadTran atmospheric model differences consists of :

- Evaluating the magnitudes differences in each LSST filter,
- Using a realistic SED catalog in spectrum shape,
- Applying apparent intensity as the test dataset.

The magnitudes are computed by calculating the flux through the effective filter transmission. The flux of a source at airmass z, in a filter band of wavelength range $\Delta\lambda$, when expressed in ADU units, is calculated by using one of the formula below :

$$F_{\Delta\lambda}^{ADU}(z, mod) = \frac{\pi D^2}{4 g_{el} hc} \int_{\Delta\lambda} T^{atm}(\lambda, z, mod) \cdot T^{opt}(\lambda) \cdot T^{filt}(\lambda) \cdot \epsilon_{CCD}(\lambda) \cdot S_{\lambda}^{E}(\lambda) \cdot \lambda \cdot d\lambda \quad (1)$$

$$F_{\Delta\lambda}^{ADU}(z, mod) = \frac{\pi D^2}{4 g_{el} h} \int_{\Delta\lambda} T^{atm}(\lambda, z, mod) \cdot T^{opt}(\lambda) \cdot T^{filt}(\lambda) \cdot \epsilon_{CCD}(\lambda) \cdot S_{\nu}^{E}(\lambda) \cdot \frac{d\lambda}{\lambda} \quad (2)$$

Then the experimental magnitudes in a filter F of passband $\Delta\lambda$ are calculated as follow :

$$M_F(mod) = -2.5 \cdot \log(F_{\Delta\lambda}) \quad (3)$$

where D, g_{el} are the telescope diameter and the electronic gain (h is the Planck constant and c is the speed of light). $S_{\lambda}^{E}(\lambda)$ or $S_{\nu}^{E}(\lambda)$ are the spectral energy distribution of the source respectively given in units $\mathrm{erg/cm^2/s/\,\mathring{A}}$ or $\mathrm{erg/cm^2/s/Hz}$. $T^{opt}(\lambda), T^{filt}(\lambda), \epsilon_{CCD}(\lambda)$ are respectively the telescope optical throughput (lens transmission and mirror reflectivity), the color filter transmission and the quantum efficiency of the CCD. For this analysis, the official throughput of the LSST telescope (Section 2.1.2) and a series of statistically representative SEDs (Section 2.1.1) are used.

The atmospheric transmission $T^{atm}(\lambda, z, mod)$ at airmass z and at wavelength λ is evaluated in Modtran ($mod = MT$) and LibRadTran ($mod = RT$).

2.1.1. SED catalog

A subset of 5000 star SEDs were randomly extracted from a generated SED catalog of 12000 samples(6). This catalog provides Pickles-like star SEDs for spectral type from

O to K, with a spectrum shape and intensity distribution representative of typical stars LSST will have in its field of view (outside the galactic plane). Figure 3 shows the set of pickles star SEDs generated for this exercise.

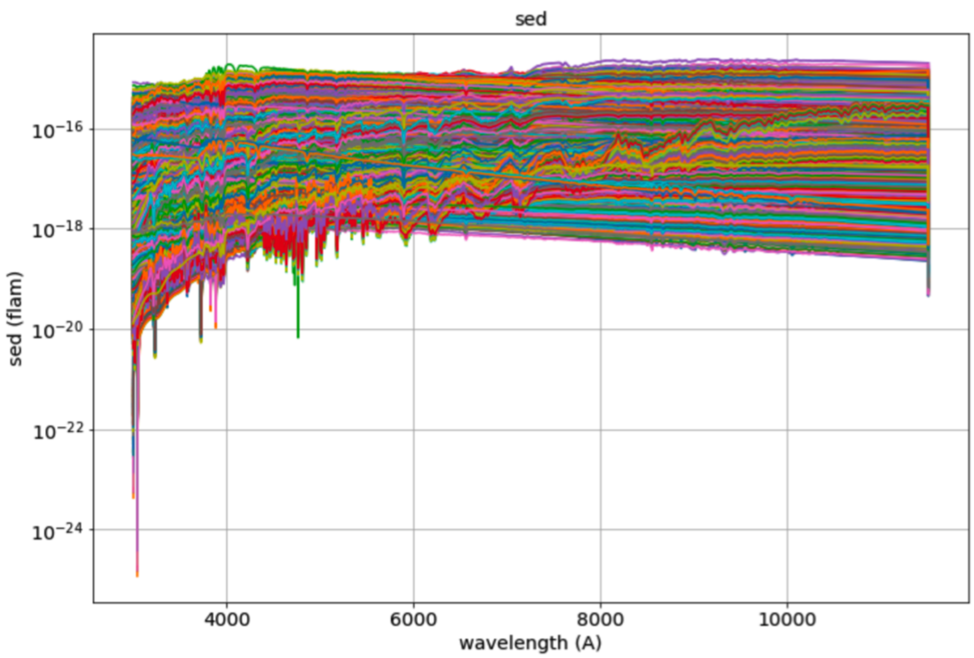

Figure 3. SED from generated Pickles-like catalog used for magnitude comparison. The flux in the vertical axis is given in $flam$ units : erg/cm^2/s/Å.

2.1.2. LSST throughputs

The effective filter transmission is the product $T^{opt}(\lambda), T^{filt}(\lambda), \epsilon_{CCD}(\lambda)$. This transmission as a function of wavelength for each filter are shown on figure 4. The filter transmissions are obtained from $lsstsims/photutils$ and provides the latest updated version of LSST transmission filters.

2.1.3. Magnitude calculation and errors

Magnitudes and their error are calculated according to the prescription in the LSST note (7), implemented in (https://github.com/lsst/sims_photUtils). The flux

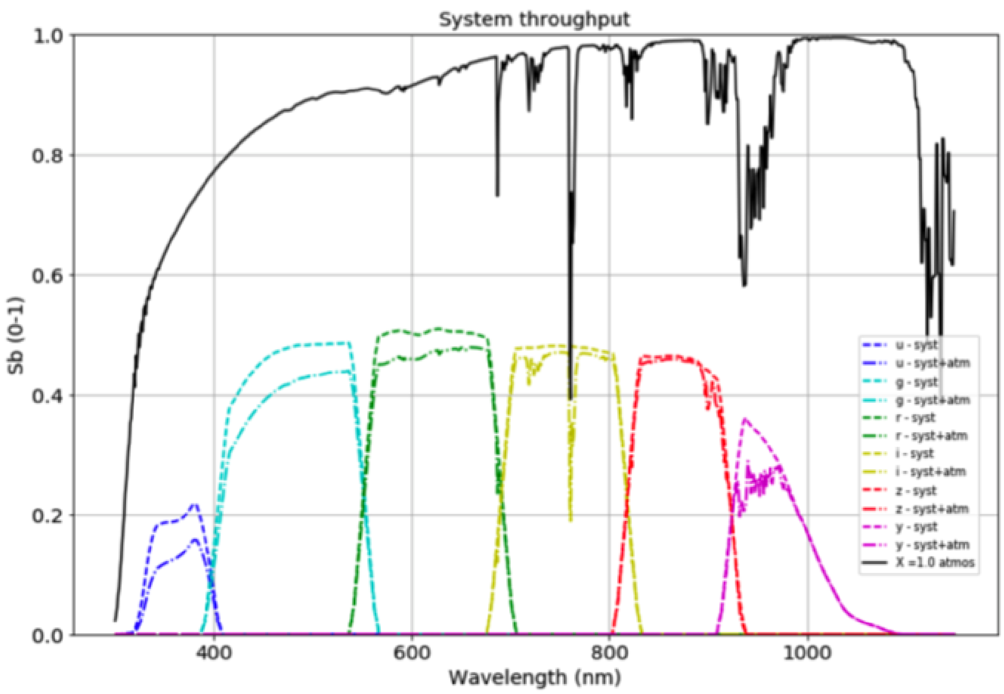

Figure 4. LSST throughput implemented in $lsstsims/photutils$.

Filter	M_F (mag/arcsec^2)
U	22.03
G	21.68
R	21.03
I	19.7
Z	17.83
Y	17.21

Table 1. Expected sky background magnitudes at LSST obtained from LSST cadence MINION1016.

through each filter depends on photoelectron statistics, sky background, seeing and exposure time (nominally 30 seconds).

These values are obtained from MINION1016 of LSST cadence for the Field Of View (FOV) (number 1000), a typical FOV outside the galactic plane. The sky-background and seeing values extracted from cadence are given in the table1 and 2.

Filter	Seeing (arcsec)
U	1.10
G	1.02
R	0.95
I	0.92
Z	0.88
Y	0.94

Table 2. Expected seeing at LSST obtained from LSST cadence MINION1016.

2.2. Parameter tuning

Beginning with a set of Modtran atmospheric transmission profiles of airmass z from 1 to 2.5 in 0.1 steps (1.a), each airmass z of Modtran transmission is estimated to give the *pwv* value and *ozone* value required in LibRadTran to get the closest magnitude in each of the filters.

2.2.1. Normalised Magnitude Residual distribution

The normalized residuals (or also called pulls) $pull_i^F(param, z)$ are defined as the magnitude difference between the Modtran and LibRadTran simulations with atmospheric parameter $param = (pwv, ozone)$ normalized by magnitude error. The SEDs are indexed by the letter i.

$$pull_i^F(param, z) = \frac{M_i^F(MT, z) - M_i^F(RT, z, param)}{\sigma(M_i^F, z)} \tag{4}$$

where $M_i^F(MT, z)$ and $M_i^F(RT, z, param)$ are respectively the magnitudes calculated by Modtran and LibRadTran by the equation 3. The magnitude error $\sigma(M_i^F, z)$ is calculated from the $lsstsims/photUils$ library.

Figure 5 shows the distribution of such pulls in Y filter at a fixed airmass z over the the entire subset of SEDs mentioned in section 2.1.1.

High values of *pwv* (red colors) induce much more absorption in LibRadTran than in Modtran and, therefore has smaller magnitudes than LibRadTran. This case is illustrated by

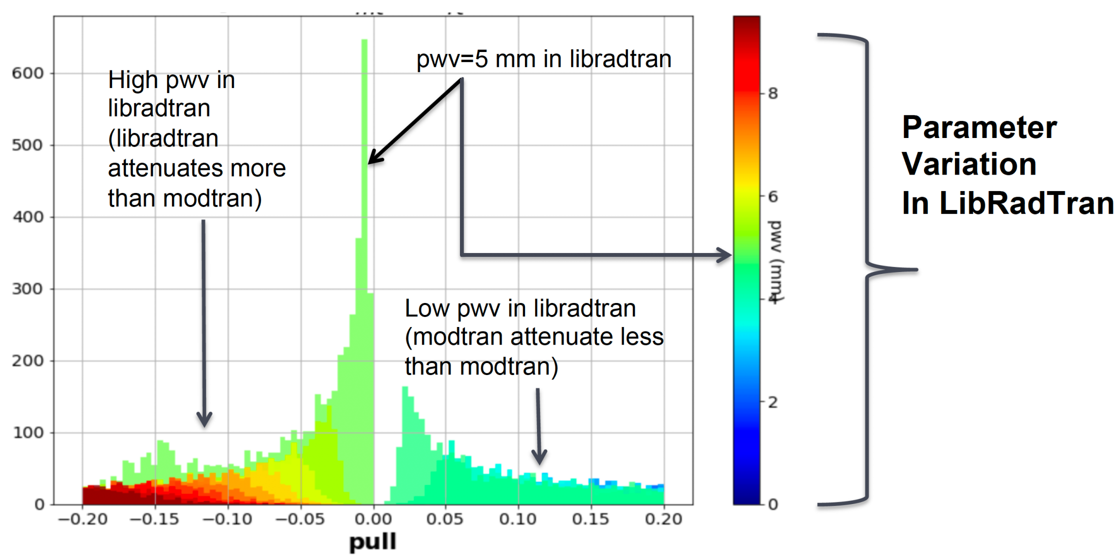

Figure 5. Example of a pull distribution in Y filter for different pwv values in LibRadTran for $z = 1.2$.

the left tails in the pulls distribution. Conversely, small *pwv* in LibRadTran, leads to less attenuation in LibRadTran than in Modtran and therefore, more positive tail pulls. LibRadTran matches perfectly with Modtran when the pulls distribution is well centered on the null value.

2.2.2. Chi-squared minimization

The optimal parameter $param_{opt}$ is found by minimizing the following $\chi^2(param, z)$ quantity which is the average sum over pulls squared. This minimization procedure is illustrated in Figure 6.

$$\chi^2(param, z) = \frac{1}{N-1} \sum_i^N \left(\frac{M_i^F(MT, z) - M_i^F(RT, z, param)}{\sigma(M_i^F, z)} \right)^2 \tag{5}$$

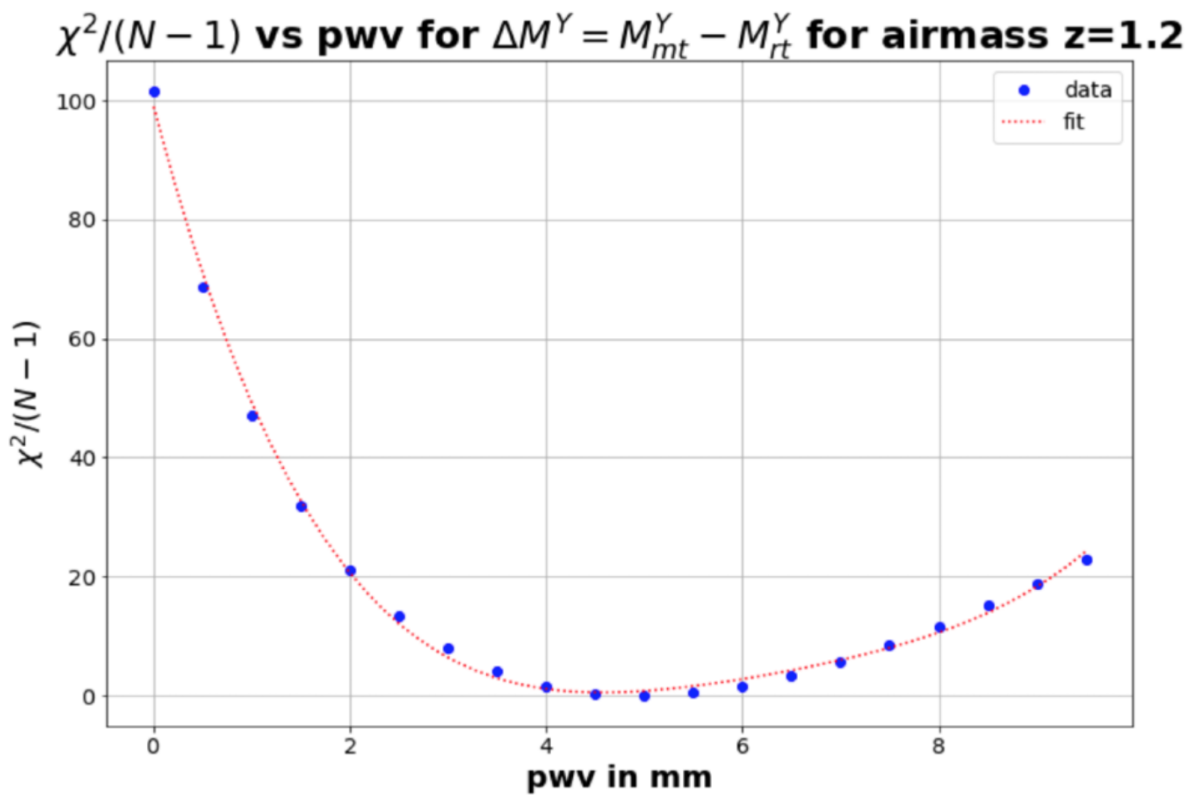

Figure 6. Example χ^2 minimization with respect to one parameter of the atmospheric model in LibRadTran.

It must be noticed that at optimum, $\chi^2(param, z)$ is almost zero instead of close to one. It can be explained because the calculation of $M_i^F(MT, z)$, $M_i^F(RT, z, param)$ has not been randomized by the magnitude error $\sigma(M_i^F, z)$. Indeed the estimate of the bias of LibRadTran compared to Modtran is needed. The pull value gives an indication on the bias value compared to the typical expected photometric error. The sensitivity on parameter tuning can be evaluated in the parameter range where $\chi^2(param, z) \leq \chi^2(param_{opt}, z) + 1$.

2.3. Tuning the precipitable water vapor parameter

The optimal value for pwv_{opt} in the Y filter is first found for each airmass value. The optimal pwv_{opt} versus airmass is shown in Figure 8.c and ranges from 4.75 mm to 5 mm. The error bars are the sensitivity in *pwv*. From this sensitivity, one can see that the variation of pwv_{opt} with airmass is not significant.

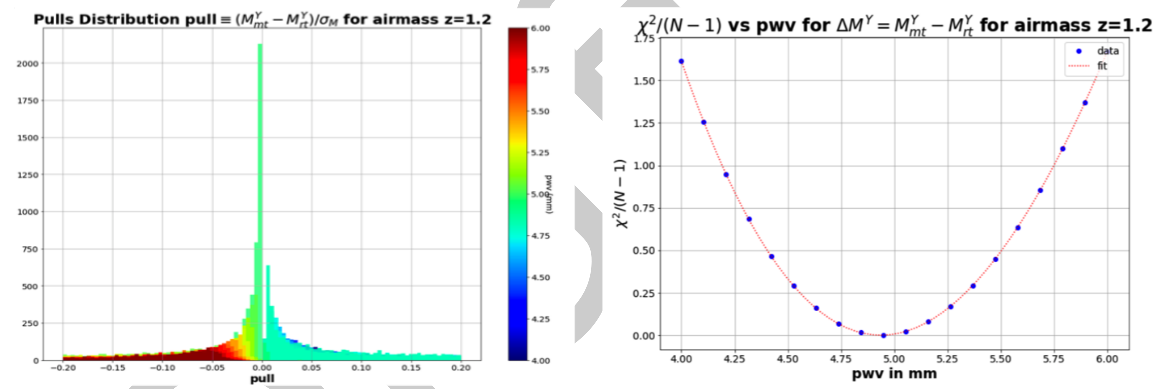

Figure 7. Tuning of precipitable water vapor parameter: a) pull distribution with respect to *pwv* (color). b) χ^2 versus *pwv*. c) Optimal *pwv*value versus airmass

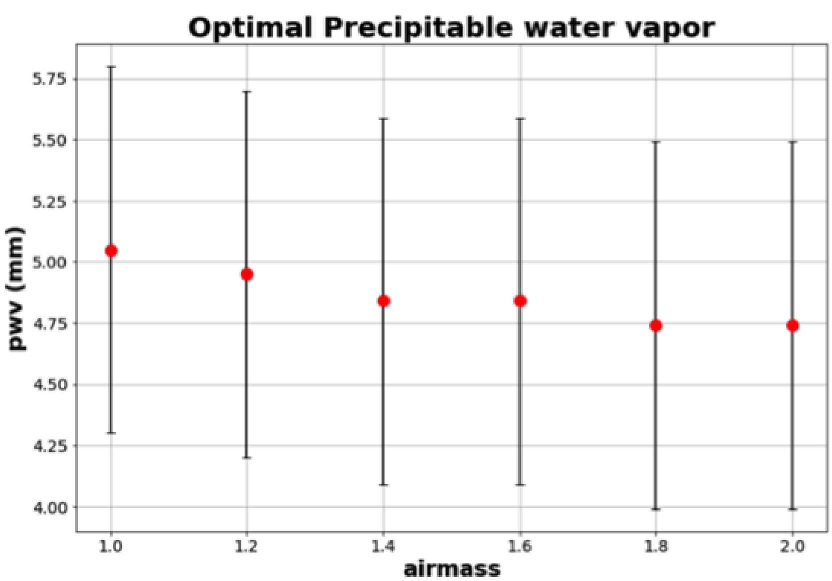

Figure 8. Optimum precipitable water vapor from χ^2 minimization versus airmass.

2.4. Tuning the precipitable ozone parameter

A similar optimization of *ozone* parameters in R filter leads to $ozone_{opt} = 340$ DbU (see Figure 9 and 10) without significant dependence with airmass.

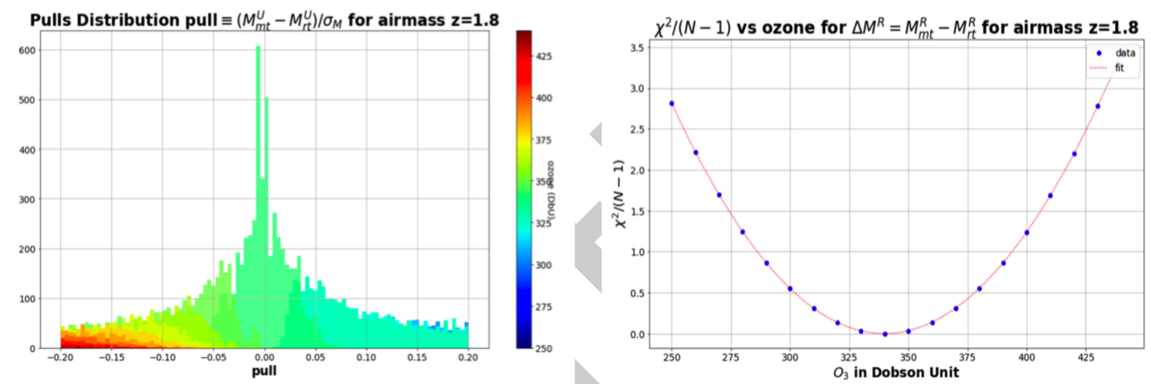

Figure 9. Tuning of *ozone* parameter : a) pull distribution with respect to *ozone* (color). b) χ^2 versus pwv.

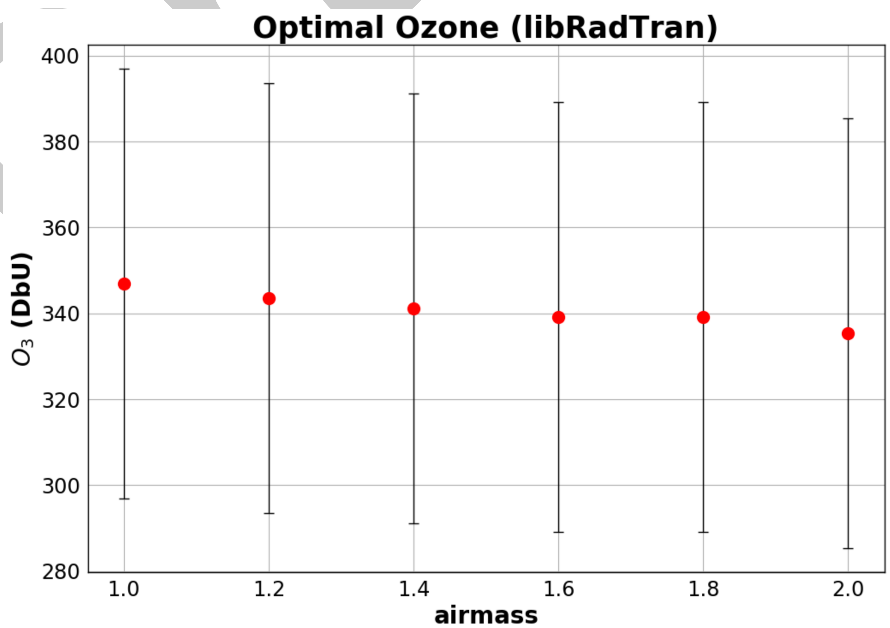

Figure 10. Optimum *ozone* parameter from χ^2 minimization versus airmass.

3. Results

3.1. Magnitude biases before any Optimization

The magnitude bias is shown on Figure 11 before adjusting any atmospheric parameter for matching magnitudes. This magnitude bias is given as a function of the SED color $G - I$ and also as a function of airmass. The default *ozone* parameter is taken to be 300 DbU and default *pwv* parameter is 4 mm in LibRadTran. For all filters, at any airmass, Modtran has a slightly lower transparency than LibRadTran (thus a positive bias in magnitude).

On the whole, the magnitude bias does not have a strong SED color dependence, but it has an airmass dependence. However, as long as this dependence is relatively contained between the two $G - I = \pm 1$ mmag lines, this bias is acceptable.

Except for the U and G band, which show an approximately 2.5 mmag bias, R, I and Z band have a bias between 5-8 mag and Y has a bias as high as 20 mmag.

The low bias in U and G is expected as the molecular scattering is the dominant light-atmosphere interaction process which is only dependent on the total atmospheric column depth. Thus a similar attenuation for the same altitude and atmospheric model (US-standard atmosphere) is expected. However, a residual *ozone* difference could explain the remaining bias, by the Huggins band effect in the U filter and by the Chappuis band effect in the G band.

It will be shown later, that the bias in R is due to Chappuis *ozone* discrepancy and the bias in Z and Y is due to *pwv* discrepancy. The most striking bias is that in the I filter. It will be shown that it is attributed to difference modelling in *oxygen* absorption.

In this note, the atmospheric parameter optimization procedure to match MT/RT magnitudes or to minimize the bias at the level or below the required accuracy (1 mmag in all filters except Y and 10 mmag for Y) is described.

An optimal atmospheric parameter search in two steps has been completed. The first step was to measure $pwv_{opt} = 5$ mm in the Y filter and the second step, was to measure $ozone_{opt}$=340 DbU in the R filter.

3.2. MT/RT Optimization of the Precipitable Water Vapor

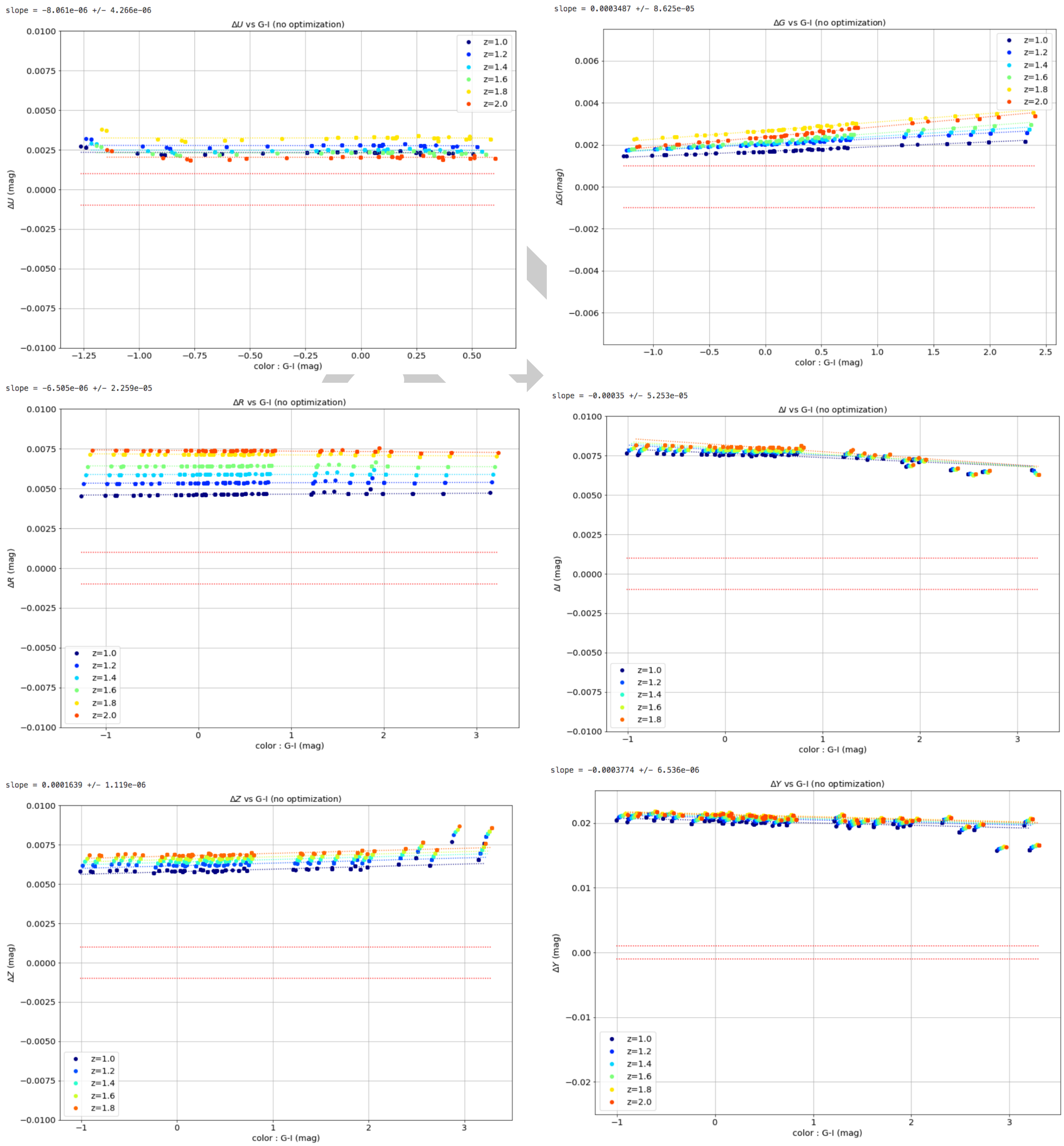

Figure 11. Magnitude bias in filters U, G, R, I, Z, Y versus SED color $G - I$, at different airmass, before any atmospheric parameter optimization.The horizontal red dotted lines give the $G - I = \pm 1$ mmag required maximum deviation.

The average magnitude bias ΔM over the SED subset in the various filters is shown in Figure 12. At this point, the Y filter has been optimized, because this band is dominated by *pwv*, and when tuned, ΔM is reduced to the order of 1 mmag for Y and Z bands (black and grey points). At this stage of the analysis, the optimization for *ozone* has not been performed yet. The magnitude biases in the R and Y and I filters are of the order of 5 mmag.

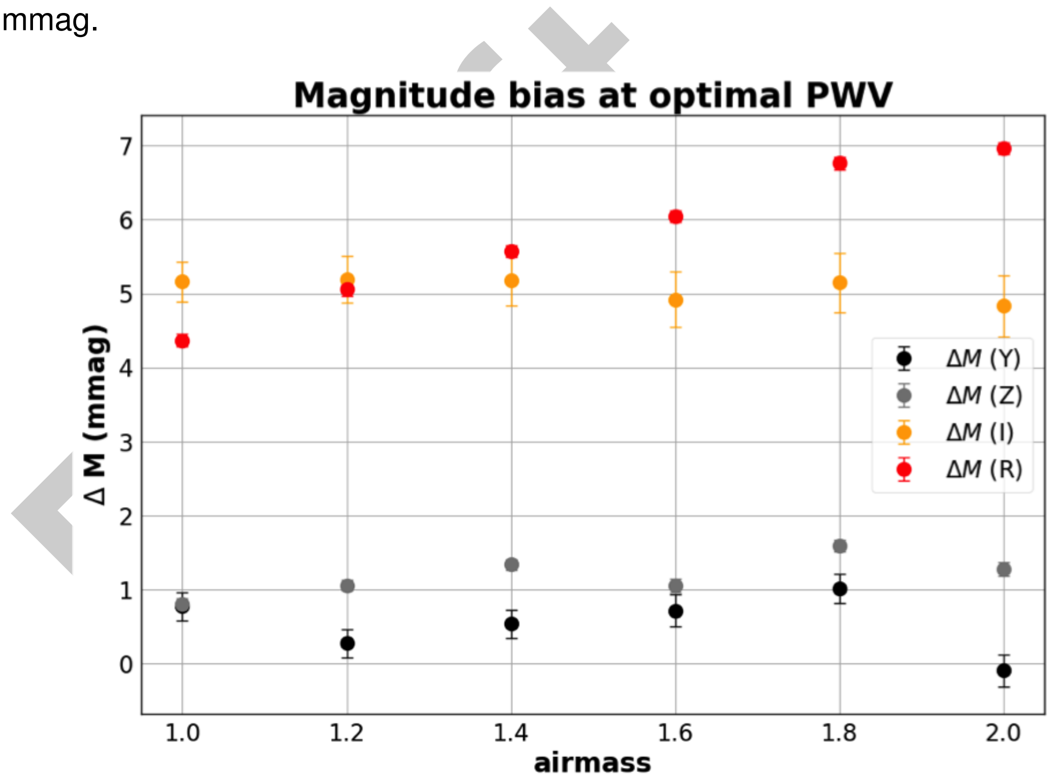

Figure 12. Magnitude bias ΔM versus airmass after tuning precipitable water vapor only. (*ozone* was not optimized yet).

The residual dependence of ΔY on SED color $G - I$ for optimized *pwv* values is shown on Figure 13. The slope $\Delta Y/(G - I)$ is as low as 0.0850 ± 0.014 mmag/mag. The vertical scale of Figure 13 is of the order of photometric errors for AB magnitudes in Y less than 17 mag.

A similar remark can be drawn for color $I - Z$ on Figure 14. The ΔY magnitude bias are well below ± 1 mmag and the the slope $\Delta Y/(I - Z)$ is as low as 0.226 ± 0.043 mmag/mag.

3.3. MT/RT Optimization of Ozone

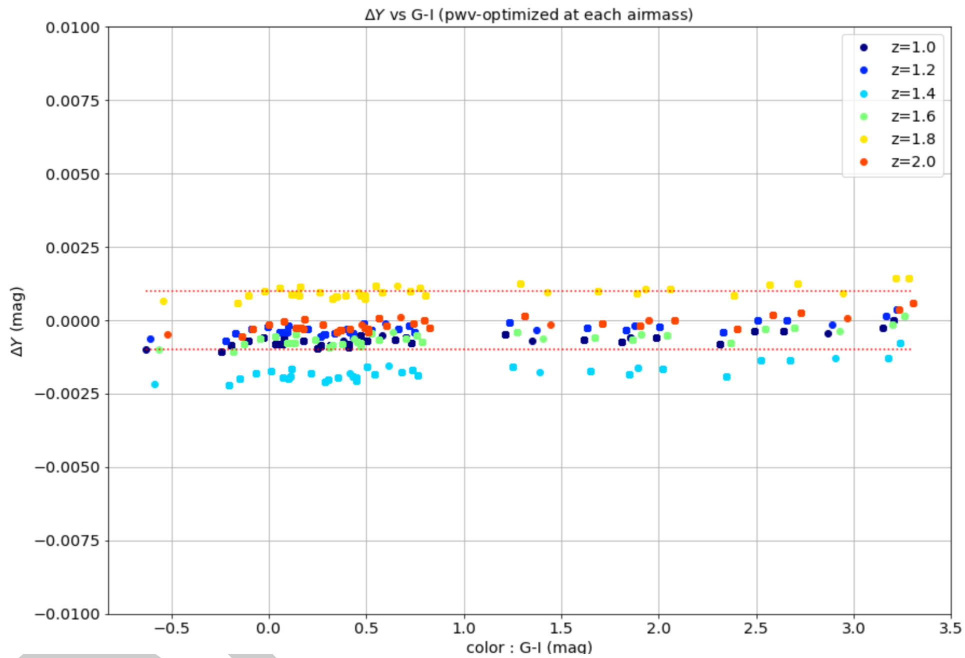

Figure 13. ΔY versus SED color $G - I$, for optimized *pwv* values. The vertical scale is of the order of photometric errors for AB-magnitudes less than 17 mag. The dotted red lines refer to a $G - I = \pm 1$ mmag bias.

.

After *ozone* optimization, the results were plotted and ΔM in filters U, G, R, I is then shown in Figure 15. The bias in G and R has been reduced below 1 mmag. The bias in the U band is about 2 mmag. It is a reasonable result for the U filter given the uncertainty on the strong atmospheric cutoff of *ozone* modelling (Huggins band).

The residual dependence of ΔR on SED color $G - I$ for optimized *ozone* values is shown on Figure 16. The slope $\Delta R/(G - I)$ is as low as 0.213 ± 0.011 mmag/mag. The vertical scale of Figure 16 is of the order of photometric errors for AB magnitudes in the I band less than 17 mag. However the bias in the I filter remains at the level 3-5 mmag which is not due to contamination from either *ozone* or precipitable water vapor. The significance of this bias is discussed in Section 4.

3.4. MT/RT Atmospheric Transmission Comparison Over the Entire Wavelength Range

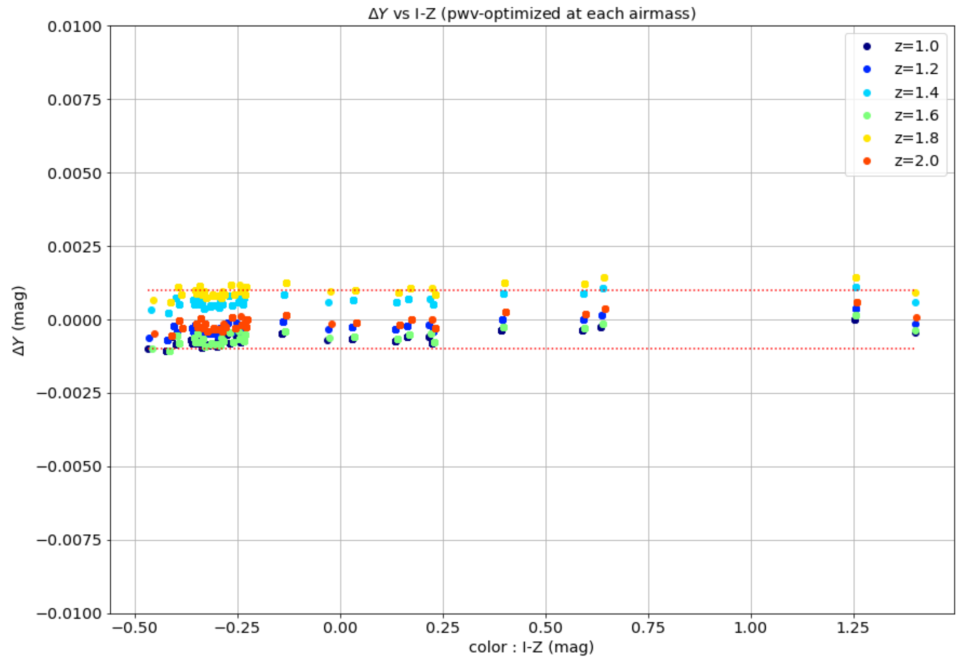

Figure 14. ΔY versus SED color $I - Z$, for optimized *pwv* values. The vertical scale is of the order of photometric errors for AB-magnitudes less than 17 mag. The dotted red lines refer to a $\Delta Y = \pm$ 1 mmag bias.

.

After parameter optimization was performed in the R and Y filters, the atmospheric transparencies of Modtran and LibRadTran were compared using an atmospheric transmission of $z = 1.2$ and is shown in Figure 17. This comparison appears to match except at the UV cutoff (the mismatch is only $\simeq$2 mmag in the U filter). A higher precision comparison can be evaluated by calculating the ratio of these transmissions. The apparent mismatch due to *pwv* is decreased after integration in the whole wavelength range in the Y filter down to a residual bias of 1 mmag.

3.5. MT/RT Comparison of the Oxygen Absorption Region

The first detailed image of the *oxygen* transmission curve is shown in Figure 18 and is the result of the analysis to investigate the *oxygen* bias in the I filter.

Different models of oxygen absorption in LibRadTran and Modtran are shown in Figure 19 demonstrate the variations and are shown below :

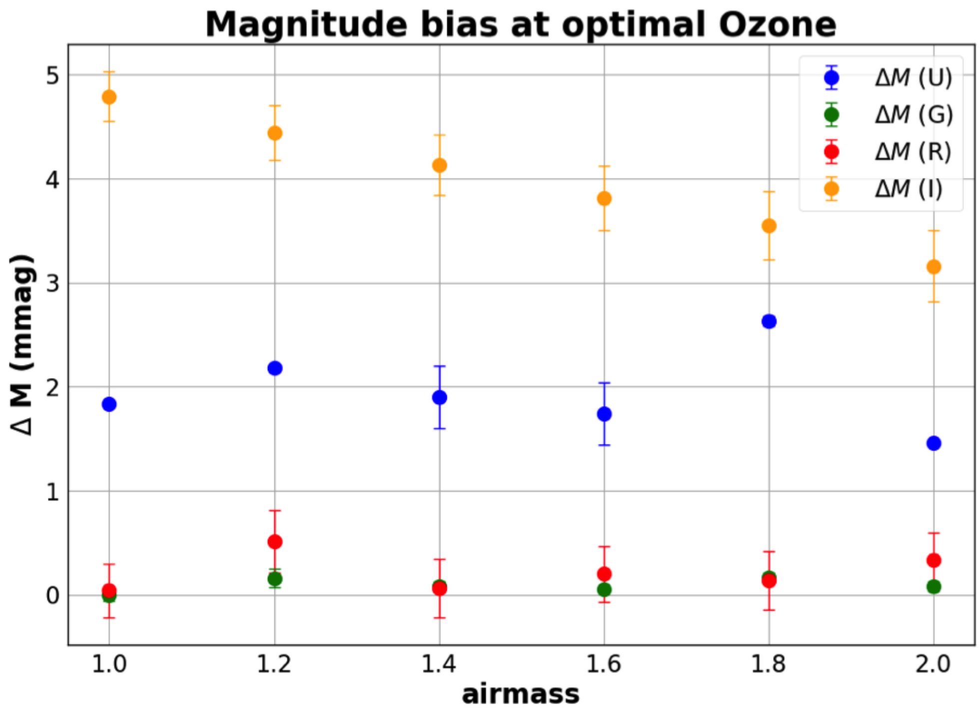

Figure 15. Magnitude bias ΔM versus airmass after tuning precipitable water vapor and *ozone*.

- radtran absorption model in LibRadTran code (RT/radtran, blue curve),
- lowtran absorption model in LibRadTran code (RT/lowtran, green curve),
- modtran model in Modtran code (MT/modtran, red curve),
- absorption model in LSSTSIM (LSSTSIM/atm, orange curve).

The *oxygen* absorption band consists of two dips. The first dip is at 761 nm and the other is at 763 nm. Clearly, the second dip has less absorption in LibRadTran compared to Modtran. For LibRadTran, the lowtran model has even less absorption than the radtran model. The second dip has an absorption height fraction which is 67.3% and 56.4% of the first dip height respectively for Modtran and LibRadTran.

The difference in the *oxygen* absorption models is responsible for the 5 mmag bias difference in the I filter between Modtran/LibRadTran. Modtran has more attenuation and this mismatch has only a 2 mmag effect in the U filter.

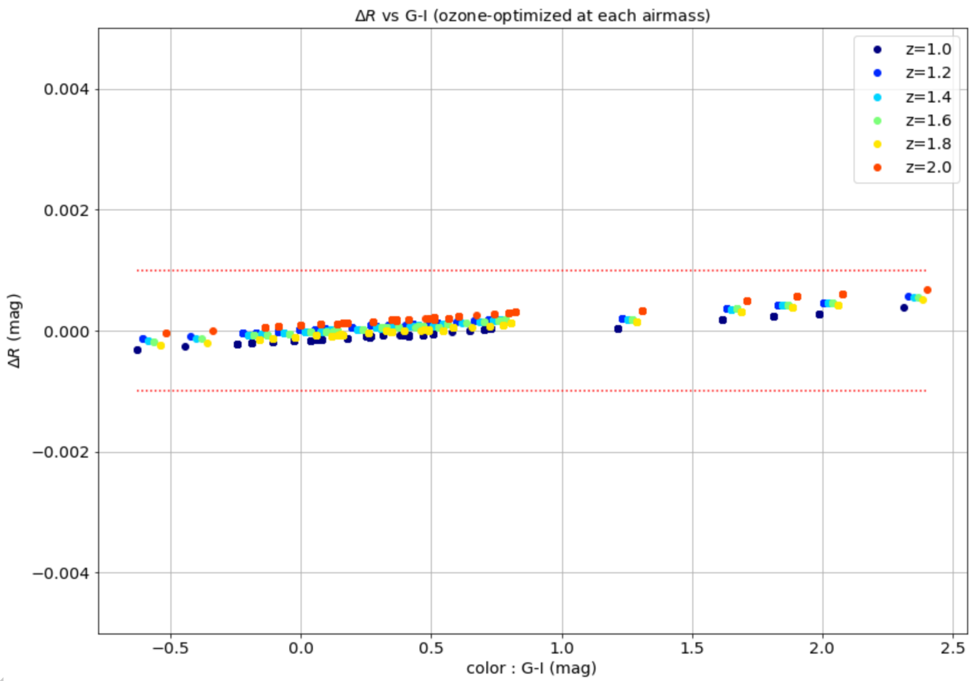

Figure 16. ΔR versus SED color, for optimized *ozone* values.The vertical scale is of the order of photometric errors for AB-magnitudes less than 17 mag. The dotted red lines refer to a $\Delta R\pm$ 1 mmag bias.

.

4. Discussion

It has been shown that Modtran and LibRadTran can predict a similar transmission profile with a residual bias on the order of 1 mmag in the G, R, Z, Y filters and 2 mmag in the U filter provided one can redefine the varying parameters by functions such :

$$\begin{cases} PWV_{RT} & = & f(PWV_{MT}) \\ ozone_{RT} & = & g(ozone_{MT}) \end{cases} \tag{6}$$

The exact knowledge of the functions f and g is not physically important. What matters is that any of the two models can be used to monitor atmospheric transparency consistently by estimating the parameters *pwv* and *ozone* over time at a different airmass. What is essential to know is that in cases using both Modtran and/or LibRadTran, monitoring over the same atmospheric transparencies, and using the same estimated values of the parameters, there is assurance that the bias differences will be less than 1 to 2 mmags. However, this is not the case in the I filter, for which the bias reaches about 5 mmag.

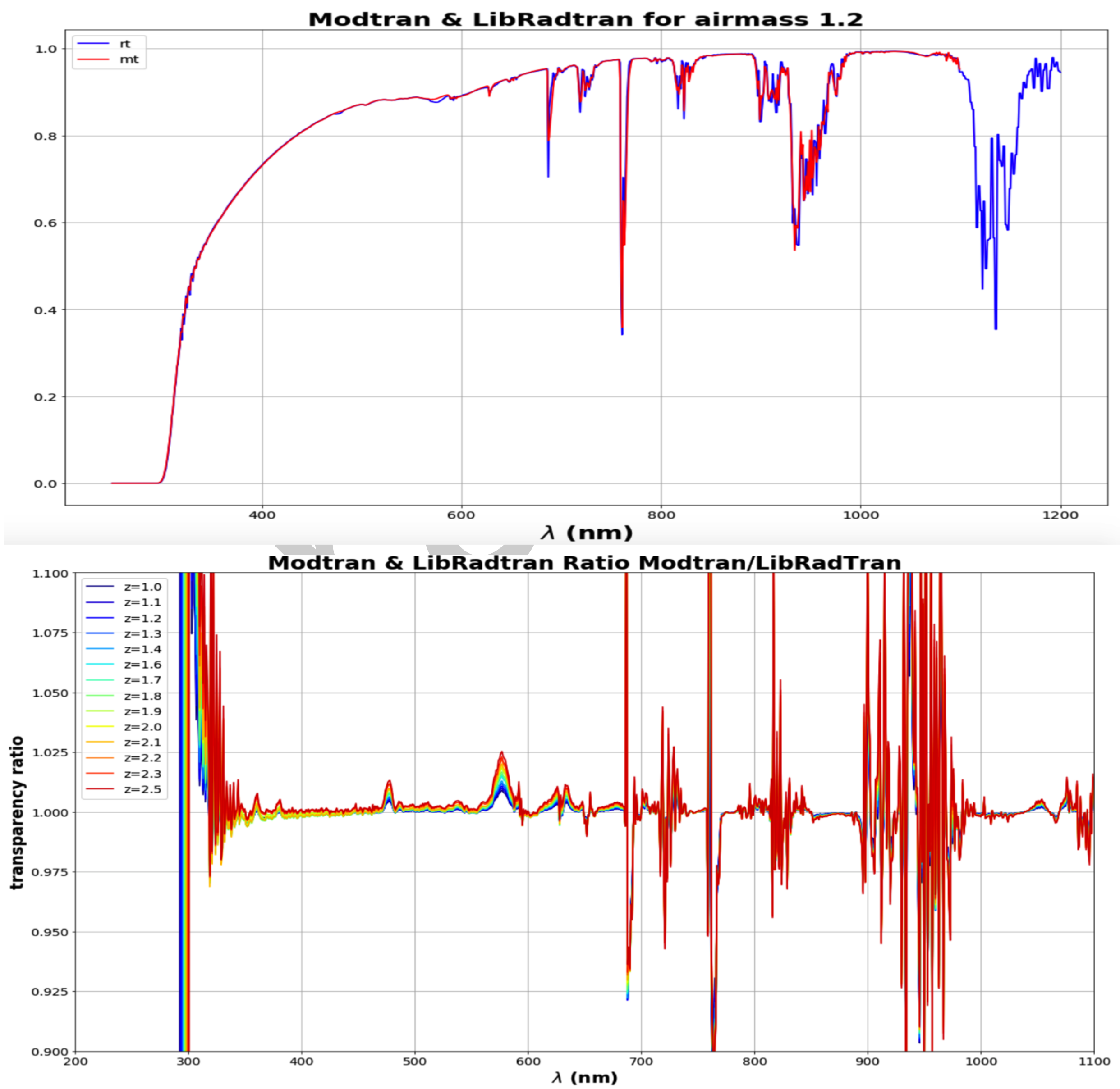

Figure 17. Comparison of atmospheric transmission after parameter tuning a) atmospheric transmission b) atmospheric transmission ratio.

4.1. The Oxygen problem

The bias in the I filter can be understood by a difference in *oxygen* absorption modelling in Modtran/LibRadTran. As shown in Figure 19.a, there is more *oxygen* absorption in

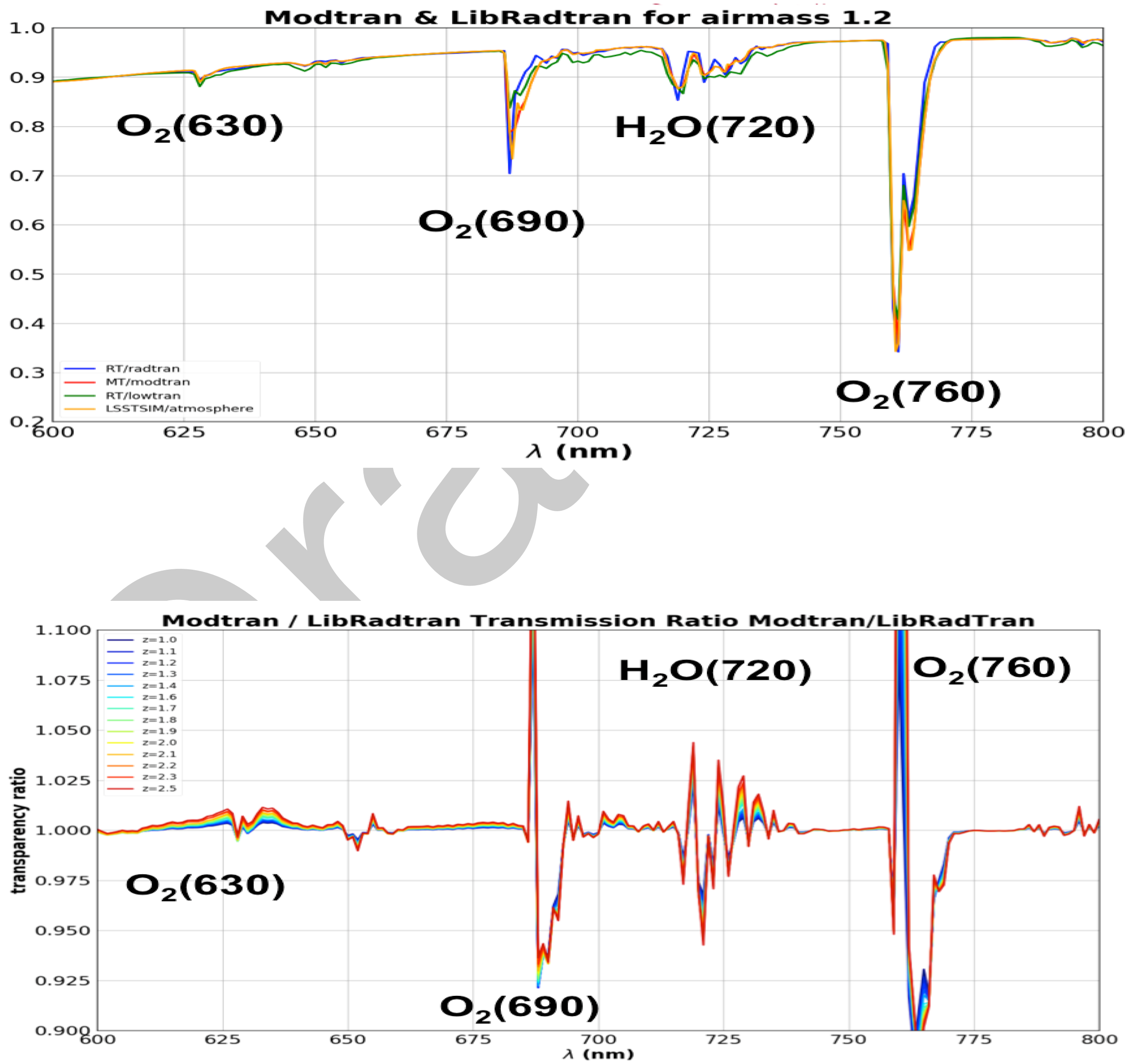

Figure 18. Comparison of atmospheric transmission in the *oxygen* absorption region after parameter tuning a) atmospheric transmission b) atmospheric transmission ratio.

Modtran than in LibRadTran. This discrepancy is inconsistent because *oxygen* density is not a model-varying parameter. Once the atmospheric pressure and temperature vertical profile is given, the air density is constrained by the perfect gas law, including the vertical

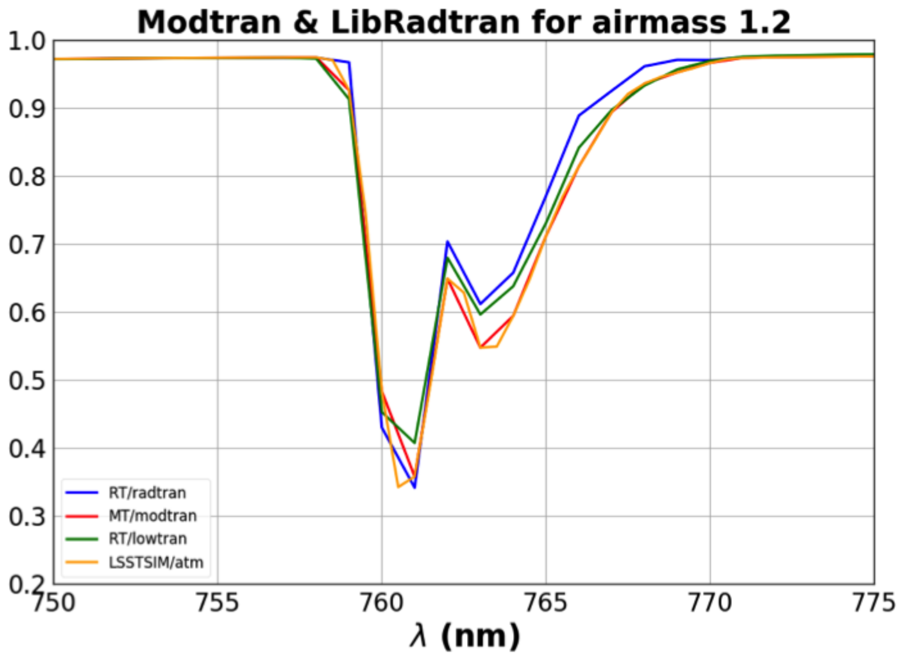

Figure 19. Main oxygen absorption band.

distribution of the dominating gas such nitrogen or *oxygen*. So the discrepancy may be attributed not to *oxygen* density but to the *oxygen* absorption modelling.

4.2. Color dependence in I filter

Similar LibRadTran I magnitudes compared to Modtran I can be recovered by increasing slightly the airmass in LibRadTran. Figure 20 shows the optimal LibRadTran airmass versus the Modtran airmass. It is found $z_{rt} \approx z_{mt} + 0.094 \pm 0.008$. Figure 21 shows the residual SED-color dependence at different airmass. Residual dependence on $G - I$ is lower than 1 mmag, thus it can be neglected.

However this airmass shift has an impact in other filters. In Figure 22, it is shown the airmass shift induces a magnitude bias of more than -16 mmag and -7 mmag in G and R band respectively. This effect is expected because increasing airmass for LibRadTran, leads a decrease of transmission in LibRadTran compared to Modtran. Thus an artificial shift of airmass must be used only in I band ,excluding this trick for other filters.

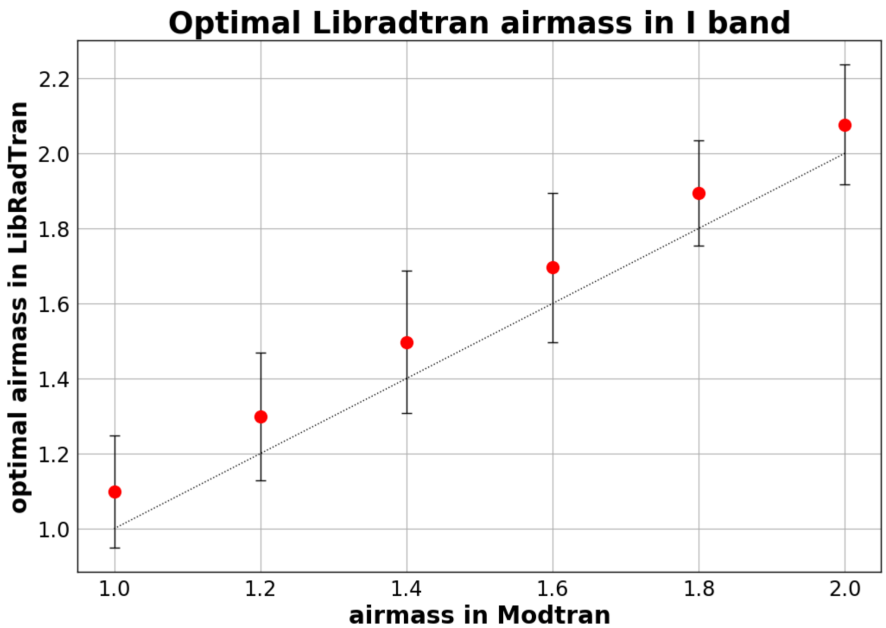

Figure 20. Optimal airmass for LibRadTran versus airmass for Modtran.

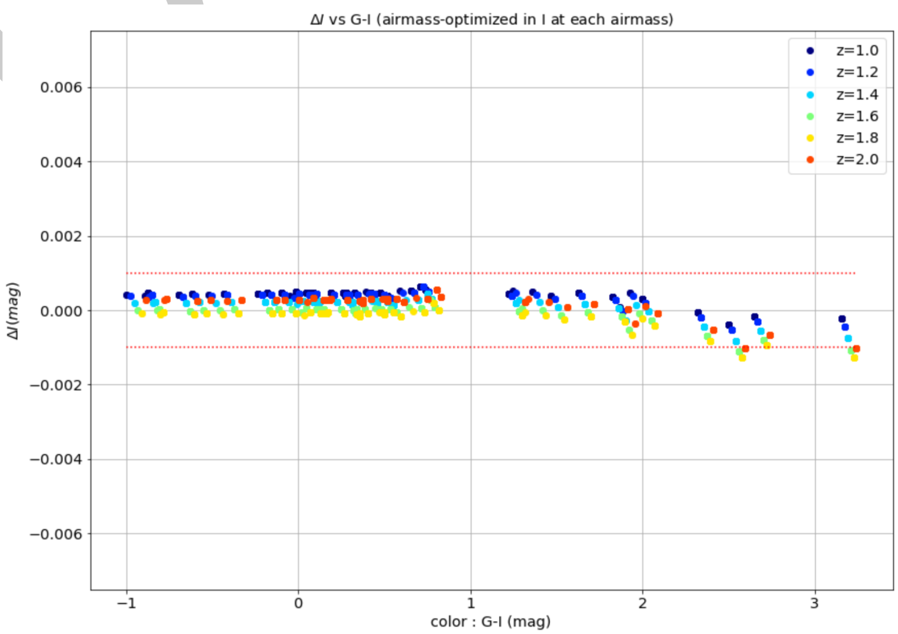

Figure 21. ΔI vs SED color. The vertical scale is of the order of photometric errors for AB-magnitudes less than 17 mag. The dotted red lines refer to a $\Delta I = \pm$ 1 mmag bias.

4.3. Hitran simulation of Oxygen absorption

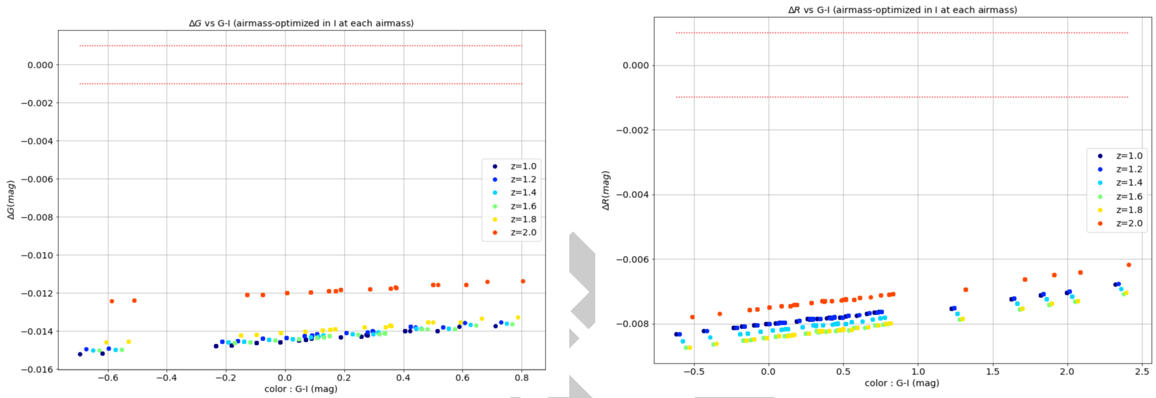

Figure 22. ΔG (left) and ΔR (right) vs SED color $G - I$ after applying the airmass shift $z_{rt} \approx z_{mt} + 0.094$. The vertical scale is of the order of photometric errors for AB-magnitudes less than 17 mag. The dotted red lines refer to a $\pm$ 1 mmag bias.

A better insight of the absorption model can be understood by reviewing the parameterization of oxygen absorption in the HITRAN spectroscopic code (1). Figure 23.a shows the absorption coefficient of oxygen in HITRAN (through its hapi interface). This absorption does not appear in a single line but in band of narrow sub-lines. The line height depends not only on temperature and pressure but also on the absorption model. When the pressure is high enough, a Lorentz profile or HT profile may be used. It is then apparent that the Lorentz profile has more absorption than a HT profile.

Also, for calculating the average transmission for a given instrument resolution in wavenumber or wavelength, the line density has to be integrated over the instrument resolution. Figure 23.b shows the transmission curve calculated for light passing through an homogeneous pure *oxygen* medium of an arbitrary fixed density and depth (Remember that the atmosphere is not an homogeneous medium). The color curves are related to the instrument resolution. The lower the instrument wavelength or wavenumber resolution, the smoother the transmission curve. For the best resolution, the transmission curve oscillates at each absorption line. For coarser resolutions, the transmission curve tends toward the magenta smooth curve for which the second dip height is a fraction of 58.8 % of the first dip height.

It is probable that a difference of *oxygen* absorption in Modtran and LibRadTran is responsible for the 5 mmag bias in the I filter.

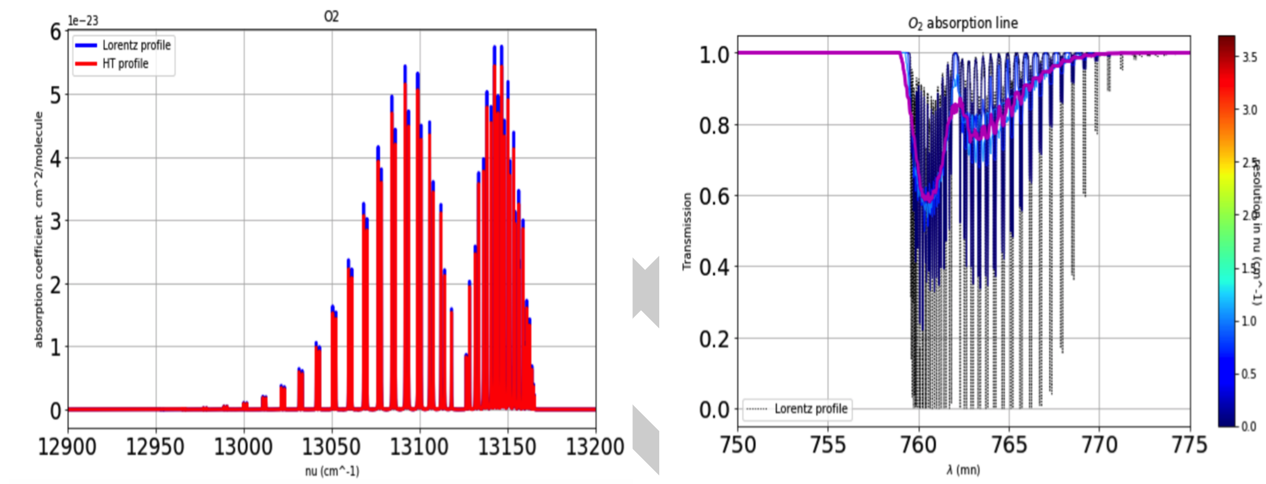

Figure 23. Calculation of molecular absorption for *oxygen* : a) Absorption coefficient per molecule in HITRAN, b) Example of calculation of oxygen transmission in air.

From the argument of the two dips ratio, we can determine HITRAN would favor the radtran model in LibRadTran compared to Modtran. However, going further to explain this difference is beyond the scope of this note.

5. Conclusion

The MT/RTanalysis in this paper was undertaken to determine if Modtran and LibRadTran predicted indistinguishable atmospheric transmission at the same airmass. It was determined that Modtran and LibRadTran have the same molecular scattering (Rayleigh) in G band, proving the atmospheric depth was similar in both codes, once the same atmospheric model US standard atmosphere" and altitude $h = 2.7$ km was chosen for a particular their configuration and using similar parameters.

It was also determined that the optimal *pwv* and *ozone* parameters in LibRadTran and Modtran predicted similar transmissions with a bias less than 1 mmag in the G, R, Z, Y filters and 2 mmag in the U filter at any airmass (relevant to the LSST Cadence airmass scan).

However it was not possible to tune such atmospheric parameter to match the I filter better than ≈ 5 mmag. We found this discrepancy was due to a specific *oxygen* absorption models disagreement between the two codes. This discrepancy can be mitigated pro-

filter	U	G	R	I	Z	Y
ΔM (mmag)	2.3	0.15	0.4	4.5/1.0	1.5	0.9

Table 3. Magnitude bias systematic error in $LSST$ filters due to atmospheric model after optimization of atmospheric parameters *pwv* and *ozone*. In the I band two values for the systematics is given, the higher corresponding to non airmass shift and the lowest one corresponding the the airmass shift $\delta z = z_{rt} - z_{mt} = +0.094$.

vided the airmass is shifted by $\delta z = 0.094$ in LibRadTran with respect to Modtran, only for the I band.

To conclude, Table 3 provides the upper systematic error on magnitudes in each filter that should be considered for an atmospheric attenuation estimation based on the use of Modtran/LibRadTran.

Except for the I filter, the magnitude bias is of the order of the calibration systematic requirements. However, it is possible to link the magnitudes in I band by artificially shifting airmass by δz in LibRadTran compared to Modtran.

Acknowledgments

lsstsim/photutils

We thanks $lsstsims/photutils$ team (https://github.com/lsst/sims_photUtils/tree/master/python/lsst/sims/photUtils).

LSST cadence

We thanks LSST cadence team (https://www.lsst.org/scientists/simulations/opsim/opsim-survey-data and https://www.lsst.org/scientists/simulations/opsim/opsim-v335-benchmark-surveys).

Author contributions are listed below.
S. Dagoret-Campagne: LibRadTran
K. Gilmore: Modtran

The DESC acknowledges ongoing support from the Institut National de Physique Nucléaire et de Physique des Particules in France; the Science & Technology Facilities Council in the United Kingdom; and the Department of Energy, the National Science Foundation, and the LSST Corporation in the United States. DESC uses resources of the IN2P3 Computing Center (CC-IN2P3–Lyon/Villeurbanne - France) funded by the Centre National de la Recherche Scientifique; the National Energy Research Scientific Computing Center, a DOE Office of Science User Facility supported by the Office of Science of the U.S. Department of Energy under Contract No. DE-AC02-05CH11231; STFC DiRAC HPC Facilities, funded by UK BIS National E-infrastructure capital grants; and the UK particle physics grid, supported by the GridPP Collaboration. This work was performed in part under DOE Contract DE-AC02-76SF00515.

References

[1]High-resolution transmission molecular absorption database (hitran), 1986 edition, 1980.

[2]A. Berk, G.P. Anderson, P.K. Acharya, E.P. Shettle. *MODTRAN5.2.0.0 USERS MANUAL*, spectral sciences, inc edition, 2008.

[3]A. Berk, G.P. Anderson, P.K. Acharya, M.L. Hoke, J.H. Chetwyn, L.S. Bernstein, E.P. Shettle, M.W. Matthew, and S.M. Adler-Golden. *MODTRAN4 Version 3 Revision 1 USERS MANUAL*, air force research laboratory edition, 2003.

[4]American National Standard,(American Institute of Aeronautics and Astronautics). Guide to reference and standard atmosphere models. Technical report, 1996. http://www.spacewx.com/Docs/AIAA_G-003B-2004.pdf.

[5]Bernhard Mayer, Arve Kylling, Claudia Emde, Robert Buras, Ulrich Hamann, Josef Gasteiger, Bettina Richter. *LibRadtran user's guide*, 2.0.1 edition, 2015.

[6]Dagoret-Campagne Sylvie. Generation of a star sed catalog. Technical report, 2018.

[7]Zeljko Ivezic, Lynne Jones, and Robert Lupton. The lsst photon rates and snr calculations. Technical report, 2010.